www.czasopisma.pan.pl PAN www.journals.pan.pl
Opto-Electronics Review 27 (2019) 219–223

Contents lists available at ScienceDirect

Opto-Electronics Review

journal homepage: http://www.journals.elsevier.com/opto-electronics review

Concepts of infrared and terahertz photodetectors based on vertical graphene van der Waals and HgTe-CdHgTe heterostructures

M. Ryzhii[a,*], T. Otsuji[b], V. Ryzhii[b,c,d,e], V. Aleshkin[f], A. Dubinov[f], V.E. Karasik[e], V. Leiman[d], V. Mitin[g], M.S. Shur[h,i]

[a] Department of Computer Science and Engineering, University of Aizu, Aizu-Wakamatsu 965-8580, Japan
[b] Research Institute of Electrical Communication, Tohoku University, Sendai 980-8577, Japan
[c] Institute of Ultra-High Frequency Semiconductor Electronics of RAS, Moscow 117105, Russia
[d] Center for Photonics and 2-D Materials, Moscow Institute of Physics and Technology, Dolgoprudny 141700, Russia
[e] Center for Photonics and Infrared Technology, Bauman Moscow State Technical University, Moscow 105005, Russia
[f] Institute for Physics of Microstructures of RAS, Nizhny Novgorod 603950, Russia
[g] Department of Electrical Engineering, University at Buffalo, Buffalo, NY 14260, USA
[h] Department of ECS Engineering, Rensselaer Polytechnic Institute, Troy, NY 12180, USA
[i] Electronics of the Future, Inc., Vienna, VA 22181, USA

ARTICLE INFO

Article history:
Received 20 December 2018
Received in revised form 23 April 2019
Accepted 2 June 2019

Keywords:
Graphene
HgTe-CdHgTe
Quantum well
Photodetector
Infrared
Terahertz

ABSTRACT

We review recently proposed concepts of infrared and terahertz photodetectors based on graphene van der Waals heterostructures and HgTe-CdHgTe quantum well heterostructures and demonstrate their potential.

Contents

1. Introduction

The gapless energy spectrum of graphene layers (GLs) enables the interband detectors of infrared (IR) and terahertz (THz) radiation (see, for example, [1–5]). The GL-based van der Waals (vdW) heterostructures [6–8] have been used for the realization of the GL-based IR photodetectors (PDs) with the improved characteristics. There are several review papers on graphene-based PDs [9–11]. The competing technology is HgTe-CdHgTe quantum well (QW) PDs. The recent progress in the fabrication of HgTe-CdHgTe QW heterostructures [12–15] has provided a further enhancement of the CdHgTe photodetector technology. These two technologies open up new opportunities for IR and THz radiation detection.

In this paper, we review the concepts of novel IR and THz PDs based on the vertical GL-based heterostructures using the interband (IB) transitions in the GLs [16–18] and on the quantum-well

* Corresponding author.
E-mail address: m-ryzhii@u-aizu.ac.jp (M. Ryzhii).

https://doi.org/10.1016/j.opelre.2019.06.002
1230-3402/

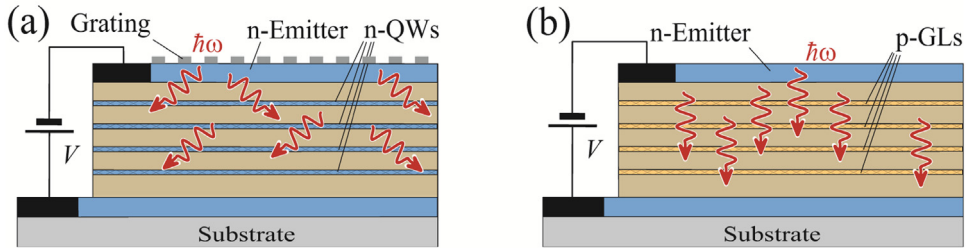

Fig. 1. Schematic view of IS-QWIP (a) and IB-GLIP (b) structures. Wavy arrows indicate the directions of the radiation propagation.

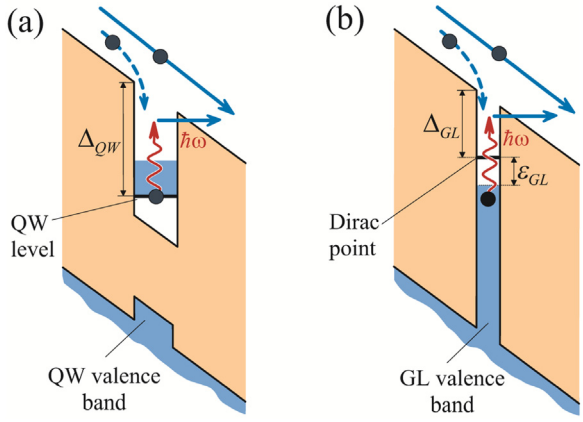

Fig. 2. Fragments of the band diagrams of IS-QWIPs (a) and IB-GLIPs (b). Wavy arrows correspond to the excitation of an electron from the QW level in the conduction band in the QWIP and from the valence band in the GLIP. Solid and dashed lines correspond to the electrons propagating in the continuum states above the barriers and those captured in the bound states, respectively.

HgTe-CdHgTe heterostructures using both the IB [19] and intersubband (IS) transitions. We also compare their characteristics.

2. Device model

Figure 1 shows the structures of the IS-QWIP (with grating providing the coupling of the incident radiation and the electrons in the QWs) and the IB-GLIP [16–18,20]. Figure 2 demonstrates the structure of the band diagrams of CdHgTe IS- and IB-QWIPs [19]. Figure 3 demonstrates the structure of the IB-QWIP and IB-GLIP both sensitive to the normally incident radiation.

The operation of the PDs under consideration is associated with the following. The infrared radiation photoexcites the electrons from the QW bound states in the IS-QWIP conduction band and from the valence band in the IB-QWIPs and IB-GLIPs to the excited states above the barrier or near the barrier top (with the consequent tunneling). In all these devices, the photoexcited electrons propagate in the continuum state of the conduction band above the barrier and reach the collector. A portion of these electrons is captured back [see the dashed arrows in Figs. 2(a), (b), and 3(b)]. The competition between the processes of photoexcitation and capture leads to the formation of the positive space charge between the emitter and the collector. This space charge stimulates the injection of the extra electrons from the emitter. The injected current can substantially exceed the current created by the photoexcited electrons (the effect of photoconductive gain), particularly, if the electron capture probability p is small [21]. The vdW heterostructures with the barrier layers made of semiconducting transition metal dichalcogenides with the electron affinities somewhat smaller than that in the GLs can be used for the GLIP under consideration. The black phosphorus and black arsenic, in which band offset Δ_{GL} ~100–200 meV, can be particularly useful as the barrier materials. The quantity Δ_{QW} in the IS-QWIPs is determined by the Cd content and the QW width d [19].

Using the device model which accounts for the processes mentioned above, we calculated the photodetector characteristics, the responsivity $R_\omega = j_\omega^{photo}/\hbar\omega I$ and the dark current limited detectivity $D_\omega^* = R_\omega/\sqrt{4egj^{dark}}$, where j_ω^{photo} and j^{dark} are the densities of the photocurrent and dark current, respectively, I is the intensity of incident radiation, e is the electron charge, $g = 1/Np$ is the photoconductive gain, and N is the number of the GLs and QWs in the device structures. These quantities were calculated using the pertinent formulas obtained by us previously [16,17].

They are shown in the consequent figures. For the definiteness, for the GLIPs we set $p = 0.01$. The coefficient of the IB photon absorption in the GLs was taken to be 2.3%. We also used the IB absorption coefficients calculated previously [19].

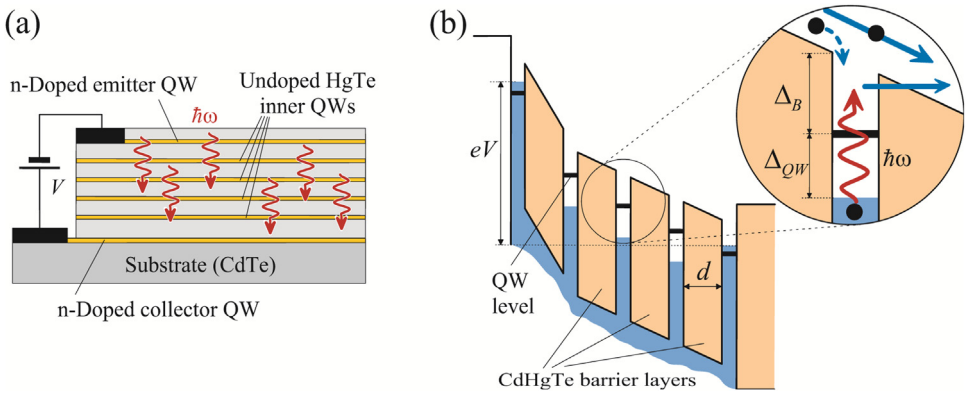

Fig. 3. Schematic view of the IB-QWIP structure (a) and its band diagram (b).

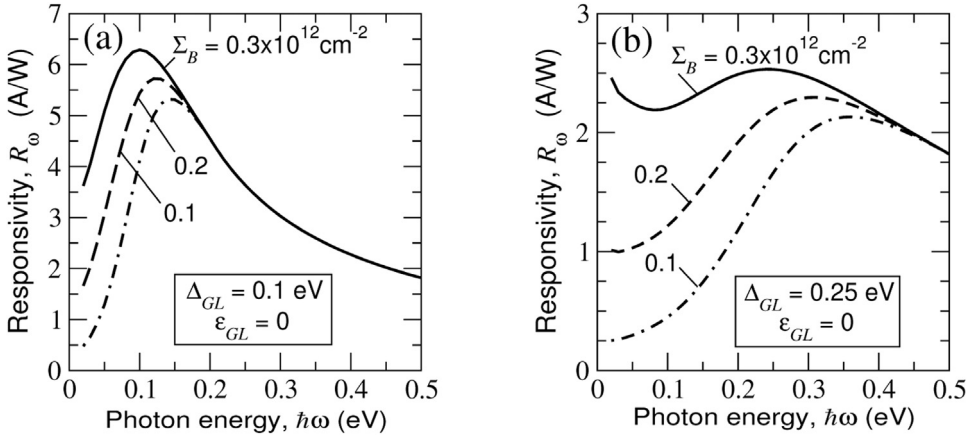

Fig. 4. Spectral characteristics of IB-GLIPs with the barrier height Δ_{GL} =0.1 eV (a) and Δ_{GL} =0.25 eV (b) for different donor and acceptor densities in the barriers Σ_B, and five undoped GLs (their Fermi energy ε_{GL} = 0) at T = 100 K.

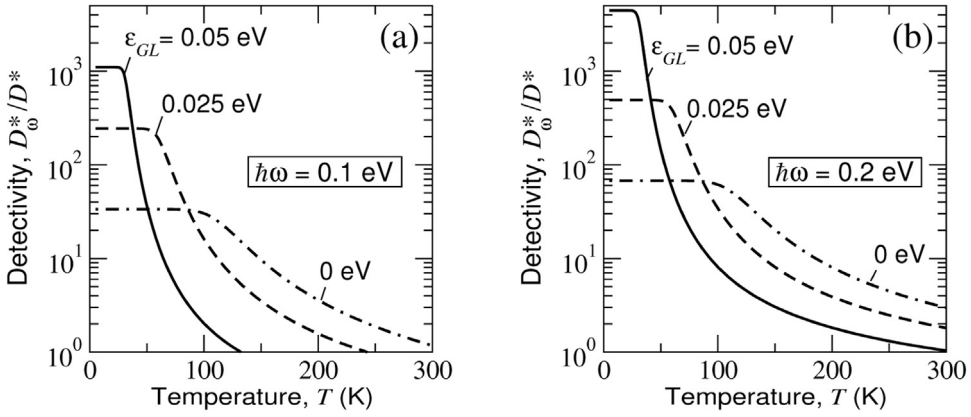

Fig. 5. The normalized IB-GLIP detectivity *vs.* temperature T at the barrier height Δ_{GL} =0.1 eV, undoped barriers and different Fermi energies ε_{GL} for different photon energies (a) $\hbar\omega$ =0.1 eV and (b) $\hbar\omega$ =0.2 eV.

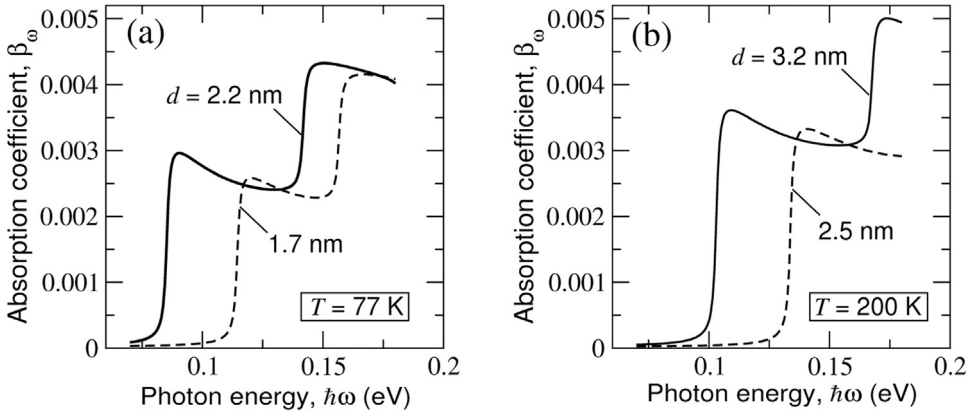

Fig. 6. The interband absorption coefficient β_ω as a function of the photon energy $\hbar\omega$ in HgTe-Cd$_x$Hg$_{1-x}$Te heterostructures with (a) x = 0.27 and width of the QW d = 2.2 and 1.7 nm at T =77 K and (b) x = 0.27 and width of the QW d = 3.2 and 2.5 nm at T =200 K.

3. Photodetector characteristics

Figure 4 shows the IB-GLIP responsivity R_ω as a function of the photon energy calculated for two values of the energy barrier Δ_{GL} at the GL - barrier material interface. As seen, the IB-GLIPs with chosen Δ_{GL} can exhibit rather high responsivities in the photon energy range from the THz to mid-IR. The plots in Fig. 4 demonstrate that the IB-GLIP spectral characteristics can be effectively modified not only by the selection of the value Δ_{GL} (i.e., by selection of the barrier material with the proper band alignment [22]), but also by doping of the GLs and the barriers. In particular, the dipole doping of the barriers could be used. Figure 5 shows the temperature dependence of the dark-current-limited detectivity, D^*_ω, of IB-GLIP at different photon energies normalized by the characteristic detectivity D^*.

The typical values of this parameter are $D^* \sim 5 \times (10^4 - 10^5)$ cm$\sqrt{\text{Hz}}$/W or higher depending on the structural parameters. As follows from Fig. 5, at sufficiently low temperatures the IB-GLIP detectivity can be fairly high: $D^*_\omega \gg D^*$.

Figure 6 shows the examples of the IB-QWIP heterostructure absorption spectra. As seen, the absorption coefficient exhibits the

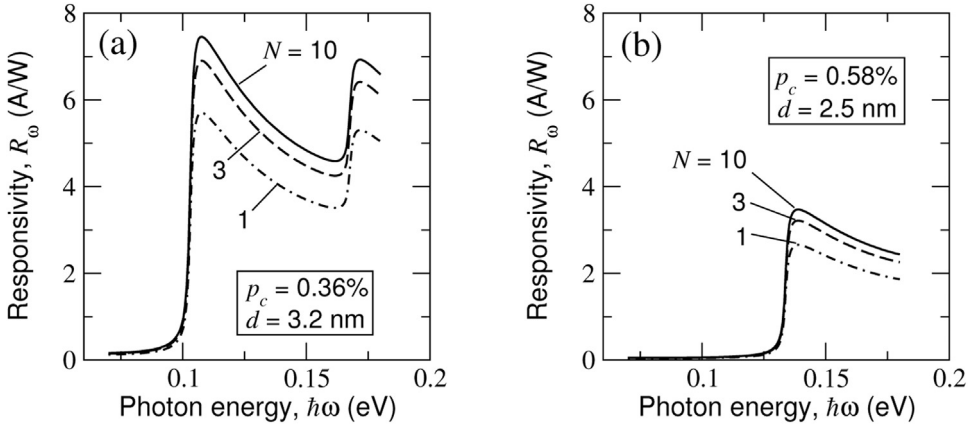

Fig. 7. The $Cd_{0.3}Hg_{0.7}Te$ IB-QWIP responsivity as a function of the photon energy $\hbar\omega$ for different number of the QWs N at temperature T =200 K: the QW width d and capture probability p_c are: (a) d =3.2 nm and p_c = 0.36% and (b) d =2.5 nm and p_c = 0.58%.

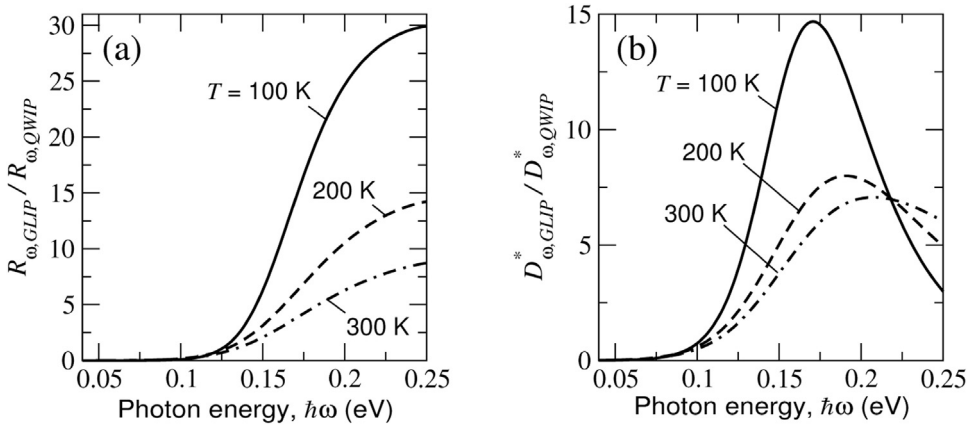

Fig. 8. Ratios of (a) the responsivities and (b) detectivities of IB-GLIPs and IS-QWIPs *vs*. the photon energy $\hbar\omega$ for different temperatures T: Δ_{GL} =0.125 eV and the hole Fermi energy ε_{GL} =0.075 eV at average electric field E = 100 V/cm.

threshold behaviour. Its two-step increase with increasing photon energy is due to the split of the hole subbands. Figure 7 shows the IB-QWIP responsivity *vs*. photon energy calculated for the device structures with different number of the QWs N. A modest increase in the responsivity with increasing number of the QWs is common for the PDs (including the IB-GLIPs, IB-QWIPs, and IS-QWIPs) based on vertical heterostructure exhibiting a sufficiently strong photoelectric gain.

Figure 8 compares the IB-GLIP and IS-QWIP responsivities and detectivities. This figure demonstrates that both responsivity and detectivity of the IB-GLIPs (being close to those in IB-QWIPs) can markedly exceed those of the IS-QWIPs. This is attributed to a much higher IB absorption coefficient than the IS absorption coefficients.

The comparison of the responsivity of the IB-GLIPs and IB-QWIPs with the responsivity of the IS-QWIPs based on the III-V QWs shows markedly higher values of the latter. This is due to smaller values of the capture probability in the IB-GLIPs and IB-QWIPs in comparison with III-V QWIPs [23]. The latter is associated with the dependence $R_\omega \tilde{1}/p$.

4. Conclusions

We considered the operation of the IB-GLIPs and IB-QWIPs and presented their characteristics. These infrared (or terahertz) PDs can exhibit the elevated performance surpassing that of the IS-QWIPs. This is due to higher efficiency of the interband processes than the intersubband processes and smaller electron capture probability in the IB-GLIPs and IB-QWIPs.

Authors statement

All authors have contributed equally to the paper.

Acknowledgements

This work was supported by the Japan Society for Promotion of Science, KAKENHI Grant No. 16H06361, the RIEC Nation-Wide Cooperative Research Project, the Russian Scientific Foundation, Grant No. 14-29-00277, the Russian Foundation for Basic Research, Grants No. 16-29-03402 and No. 18-52-50024, and the US Office of Naval Research.

References

[1] T. Mueller, F.N.A. Xia, P. Avouris, Graphene photodetectors for high-speed optical communications, Nat. Photon. 4 (2010) 297–301.
[2] F. Bonaccorso, Z. Sun, T. Hasan, A.C. Ferrari, Graphene photonics and optoelectronics, Nat. Photon. 4 (2010) 611–622.
[3] V. Ryzhii, M. Ryzhii, V. Mitin, T. Otsuji, Terahertz and infrared photodetection using p-i-n multiple-graphene-layer structures, J. Appl. Phys. 107 (2010), 054512.
[4] V. Ryzhii, N. Ryabova, M. Ryzhii, N.V. Baryshnikov, V.E. Karasik, V. Mitin, T. Otsuji, Terahertz and infrared photodetectors based on multiple graphene layer and nanoribbon structures, Opto-Electron. Rev. 20 (2012) 15–25.
[5] A. Tredicucci, M.S. Vitielo, Device concepts for graphene-based terahertz photonics, IEEE J. Sel. Top. Quantum Electron. 20 (1) (2014), 8500109.
[6] A.K. Geim, I.V. Grigorieva, Van der Waals heterostructures, Nature 499 (2013) 419–425.
[7] F. Xia, H. Wang, Di Xiao, M. Dubey, A. Ramasubramaniam, Two-dimensional material nanophotonics, Nat. Photon. 8 (2014) 899–907.

[8] D. Spirito, D. Coquillat, S.L. De Bonis, A. Lombardo, M. Bruna, A.C. Ferrari, V. Pellegrini, A. Tredicucci, W. Knap, M.S. Vitiello, High performance bilayer-graphene terahertz detectors, Appl. Phys. Lett. 104 (6) (2014), 061111.
[9] F.H.L. Koppens, T. Mueller, P.h. Avouris, A.C. Ferrari, M.S. Vitiello, M. Polini, Photodetectors based on graphene, other two-dimensional materials and hybrid systems, Nat. Nanotechnol. 9 (2014) 780–793.
[10] M. Casalino, U. Sassi, I. Goykhman, A. Eiden, E. Lidorikis, S. Milana, D. De Fazio, F. Tomarchio, M. Iodice, G. Coppola, A.C. Ferrari, Vertically illuminated, resonant cavity enhanced, graphene–silicon schottky photodetectors, ACS Nano 11 (11) (2017) 10955–10963.
[11] W. Xiaomu, G. Xuetao, Graphene integrated photodetectors and opto-electronic devices – a review, Chin. Phys. B 26 (3) (2017), 034203.
[12] S. Dvoretsky, N. Mikhailov, Y. Sidorov, V. Shvets, S. Danilov, B. Wittman, S.D. Ganichev, Growth of HgTe quantum wells for IR to THz detectors, J. Electron. Mater. 39 (7) (2010) 918–923.
[13] S. Morozov, V. Rumyantsev, M. Fadeev, M. Zholudev, K. Kudryavtsev, A. Antonov, A. Kadykov, A. Dubinov, V. Gavrilenko, N. Mikhailov, S. Dvoretsky, Stimulated emission from HgCdTe quantum well heterostructures at wavelengths up to 19.5 μm, Appl. Phys. Lett. 111 (19) (2017), 192101.
[14] S. Ruffenach, A. Kadykov, V.V. Rumyantsev, J. Torres, D. Coquillat, D. But, S.S. Krishtopenko, C. Consejo, W. Knap, S. Winner, M. Helm, M.A. Fadeev, N.N. Mikhailov, S.A. Dvoretzky, V.I. Gavrilenko, S.V. Morozov, F. Teppe, HgCdTe-based heterostructures for terahertz photonics, APL Mater. 5 (3) (2017), 035503.
[15] Q. Chen, M. Sanderson, C. Zhang, Nonlinear terahertz response of HgTe/CdTe quantum wells, Appl. Phys. Lett. 107 (8) (2015), 081111.
[16] V. Ryzhii, M. Ryzhii, D. Svintsov, V. Leiman, V. Mitin, M.S. Shur, T. Otsuji, Infrared photodetectors based on graphene van der Waals heterostructures, Infrared Phys. Technol. 84 (2017) 72–81.
[17] V. Ryzhii, M. Ryzhii, D. Svintsov, V. Leiman, V. Mitin, M.S. Shur, T. Otsuji, Nonlinear response of infrared photodetectors based on van der Waals heterostructures with graphene layers, Opt. Express 25 (5) (2017) 5536–5549.
[18] V. Ryzhii, M. Ryzhii, V. Leiman, V. Mitin, M.S. Shur, T. Otsuji, Effect of doping on the characteristics of infrared photodetectors based on van der Waals heterostructures with multiple graphene layers, J. Appl. Phys. 122 (5) (2017), 054505.
[19] V. Ya. Aleshkin, A.A. Dubinov, S.V. Morozov, M. Ryzhii, T. Otsuji, V. Mitin, M.S. Shur, V. Ryzhii, Interband infrared photodetectors based on HgTe-CdHgTe quantum-well heterostructures, Opt. Mater. Express 8 (5) (2018) 1349–1358.
[20] V. Ryzhii, T. Otsuji, V.E. Karasik, M. Ryzhii, V. Leiman, V. Mitin, M.S. Shur, Comparison of intersubband quantum-well and interband graphene-layer infrared photodetectors, IEEE J. Sel. Top. Quantum Electron. 54 (2) (2018), 4000108.
[21] H. Schneider, H.C. Liu, Quantum Well Infrared Photodetectors: Physics and Applications, Springer, Berlin, 2007.
[22] G. Gong, H. Zhang, W. Wang, L. Colombo, R.M. Wallace, K. Cho, Band alignment of two-dimensional transition metal dichalcogenides: application in tunnel field effect transistors, Appl. Phys. Lett. 103 (5) (2013), 053513.
[23] V. Ya. Aleshkin, A.A. Dubinov, M. Ryzhii, V. Ryzhii, T. Otsuji, Electron capture in van der Waals graphene-based heterostructures with WS_2 barrier layers, J. Phys. Soc. Japan 84 (2015), 094703.